Appl Phys B
DOI 10.1007/s00340-009-3732-4

Applied Physics B
Lasers and Optics

Diode-end-pumped $Tm:GdVO_4$ laser operating at 1818 and 1915 nm

M.J.D. Esser · D. Preussler · E.H. Bernhardi · C. Bollig · M. Posewang

Received: 8 February 2009 / Revised version: 31 July 2009

Abstract High power operation at 1818 and 1915 nm has been demonstrated from a $Tm:GdVO_4$ laser operating in quasi-continuous-wave mode with a maximum measured power of 8.7 W and a laser output energy of 175 mJ was observed in a 20 ms pulse at 1.9 µm. The operation at 1818 nm is the shortest wavelength achieved at multi-watt power levels for a Tm-doped solid-state laser without intra-cavity tuning elements. It has been shown that by careful analysis of the emission spectra, the $Tm:GdVO_4$ laser can be tuned over a 100 nm wavelength range simply by appropriate selection of the reflectivity of the output coupler.

PACS 42.55.-f · 42.55.Xi · 42.60.By · 42.70.Hj

1 Introduction

There has been considerable interest in the use of orthovanadates as host crystals for rare-earth-doped diode-pumped solid-state lasers, including Tm^{3+}-doped vanadate crystals, which have been shown to exhibit certain advantages over other host crystals [1]. In particular, $Tm:YVO_4$, $Tm:LuVO_4$ and $Tm:GdVO_4$ all have strong and broad absorption features at the emission wavelength of commercially available high-power laser diodes at ∼800 nm [2]. The broad emission peak at 1.9 µm in $Tm:GdVO_4$ can be utilised for laser operation over a useful wavelength tuning range, including wavelengths which can be used to pump Ho^{3+} lasers [3]. Furthermore, $Tm:GdVO_4$ has satisfactory thermal conductivity [4, 5] and overall is an attractive gain-material option for the design of high-power diode-pumped laser devices at 1.9 µm, also considering the 2-for-1 pumping process in Tm^{3+}. However, despite its clear potential, to date there has been only limited reported success in achieving multi-watt output power with significant tunability with $Tm:GdVO_4$ lasers [6, 7].

The highest laser output power was reported by Li et al. who achieved a maximum continuous-wave output power of 2.8 W from a diode-end-pumped $Tm:GdVO_4$ laser [6]. In addition, with the use of an intra-cavity birefringent filter, they demonstrated a tuning range of 126 nm (1820 to 1946 nm). However, a broader tuning range of 235 nm (1840 to 2075 nm) has been achieved at lower power, with 1.1 W output power demonstrated at 1920 nm when tuned with an intra-cavity birefringent filter [7]. Thus even though significant wavelength tuning has been demonstrated for $Tm:GdVO_4$, the entire spectral gain has not been fully utilised to achieve multi-watt output at 1.8 µm.

In this paper we report on the design and operation of a diode-end-pumped $Tm:GdVO_4$ laser operated in a quasi-continuous-wave (QCW) mode with more than 8 W output power during the 10 to 20 ms on time of the pulse. These high QCW power levels were demonstrated with the laser wavelength centred both at 1915 and 1818 nm, without the use of a tuning element in the laser cavity. Rather, wavelength selection has been achieved by appropriate selection of the resonator output coupling value based on an analysis of spectroscopic data.

M.J.D. Esser (✉) · D. Preussler · E.H. Bernhardi · C. Bollig
National Laser Centre, Council for Scientific and Industrial Research, P.O. Box 395, Pretoria 0001, South Africa
e-mail: desser@csir.co.za
Fax: +27-12-8413152

M. Posewang
Institute of Laser-Physics, University of Hamburg, Luruper Chaussee 149, 22761 Hamburg, Germany

Published online: 15 September 2009

2 Laser design

In order to optimise the design of a high-power diode-pumped $Tm:GdVO_4$ laser that fully utilises the broad emission spectrum, a detailed spectroscopic study of the laser material is required. However, it had been found that prior to this work the spectral data available in the literature for $Tm:GdVO_4$ were not sufficiently precise to enable accurate predictions of the laser performance to be carried out, especially at longer wavelengths. We therefore embarked on accurately measuring absorption spectra of $Tm:GdVO_4$ laser crystals at both 0.8 (pump band) and at 1.9 μm (emission band). The measurements were conducted with a Cary 5000 spectrometer with resolution set to 1 nm and an integration time of 0.1 s. The $Tm:GdVO_4$ crystals, obtained from a commercial supplier (Crystech Inc, China), were used for both the spectroscopic investigations and the subsequent laser experiments. According to the supplier, the Czochralski-grown crystals had an atomic doping concentration of 3.0% while the dimensions of the laser crystals were 2.5 × 2.5 mm^2 in cross section and 3 mm in length, and the crystal for spectroscopic measurements was 10 mm long.

The absorption cross-section data (σ_{abs}) of $Tm:GdVO_4$, measured for the π-polarisation ($\boldsymbol{E}\|c$) and the σ-polarisation ($\boldsymbol{E}\perp c$) in the 1.9 μm wavelength region, are shown in Fig. 1. A running average over 6 nm was applied to the data to reduce the noise. During the spectroscopic measurements the total transmission was less than 1% for the π-polarisation between 1735 and 1820 nm through the 10 mm crystal, which makes the cross-section data less reliable in this region. Also presented in Fig 1 are data for the emission cross sections, σ_{em} of the $^3F_4$–$^3H_6$ laser transition at 1.9 μm, which were calculated by the reciprocity method from the smoothed and offset-corrected absorption cross-section data [8].

The absorption and emission cross-section data as depicted in Fig 1 are in good agreement with previously reported data [2]. On both polarisations the peak absorption is located at around 1750 nm, and the peak emission occurs between 1810–1820 nm, with the peak cross sections of the π-polarisation always stronger. The π-polarisation emission cross section has a smooth decay towards longer wavelengths, while on the σ-polarisation the emission cross section has distinct spectral features located at 1850 and at 1910 nm. These accurately measured absorption spectra, and the calculated emission spectra, are of crucial importance for the calculation of the expected threshold power and the operational wavelength of the $Tm:GdVO_4$ laser.

The pump power required to achieve oscillation threshold for a diode-end-pumped $Tm:GdVO_4$ quasi-three-level laser can be calculated from the values of the absorption and emission cross section, σ_{abs} and σ_{em} using the approach developed in [9] and further extended in [10] to yield the expression,

$$P_{\text{th}}(\lambda) = \frac{\pi h\nu_p(w_l^2 + w_p^2)}{4\tau\eta_{p-q}\sigma_{\text{em}}(\lambda)}\left[L + T + 2Nl\sigma_{\text{abs}}(\lambda)\right], \tag{1}$$

where T is the transmission loss of the output coupler; L represents additional resonator losses, assumed to be 1% which is typical for a two-mirror resonator; w_l and w_p are the laser mode and pump beam radii in the laser crystal; N is the concentration of Tm^{3+} ions in the laser crystal (3 at.% doping × 1.21 × 10^{22} cm^{-3} [11]); ν_p is the frequency of the pump light; η_{p-q} is the pump quantum efficiency, typically assumed to be 1.5 for diode-pumped Tm^{3+} lasers to incorporate the 2-for-1 pumping process; σ_{abs} and σ_{em} are the absorption and the emission coefficients, respectively; τ is the lifetime of the $^3F_4$ upper laser manifold, taken as 1.85 ms [2]; and l is the length of the laser crystal, which was 3 mm.

The laser was designed for end pumping with the pump beam and the laser mode of equal size ($w_l \approx w_p \approx w$) in the crystal. The expression for the threshold power can then easily be converted to an expression of the threshold power density as follows:

$$P_{\text{th\_density}}(\lambda) = \frac{P_{\text{th}}}{\pi w^2} = \frac{h\nu_p[L + T + 2Nl\sigma_{\text{abs}}(\lambda)]}{2\tau\eta_{p-q}\sigma_{\text{em}}(\lambda)}. \tag{2}$$

By plotting $P_{\text{th\_density}}$ against wavelength for different values of output coupling T, the threshold power density required to establish lasing can be determined, as shown in Fig. 2. Furthermore, it can be assumed that for a particular output coupling value T, continuous-wave laser oscillation will occur at the wavelength and polarisation for which the threshold power density is a minimum [10]. This method of analysing a laser material for laser performance is complimentary to the "effective emission cross section" method used by other authors [2, 12]. The method used here provides the laser designer with a clear indication on the expected laser threshold pump-power density, wavelength and polarisation of the laser.

The calculations presented in Fig. 2 indicate that for a 3.0% doped, 3 mm of length $Tm:GdVO_4$ crystal laser threshold can be attained with realistic values of resonator output coupling and pump beam focussing. The predicted threshold power density for a 5% transmission output coupler is ∼28 W/mm^2 at 1912 nm, and it will naturally lase on σ-polarisation. Similarly, the predicted oscillation wavelength for the case of 20% output coupler transmission is approximately at 1855 nm with a threshold power density of ∼47 W/mm^2, also on σ-polarisation. At a high output coupler transmission of 72%, the expected threshold power density is ∼87 W/mm^2 while the predicted wavelength is 1820 nm on π-polarisation. It was concluded that the slight

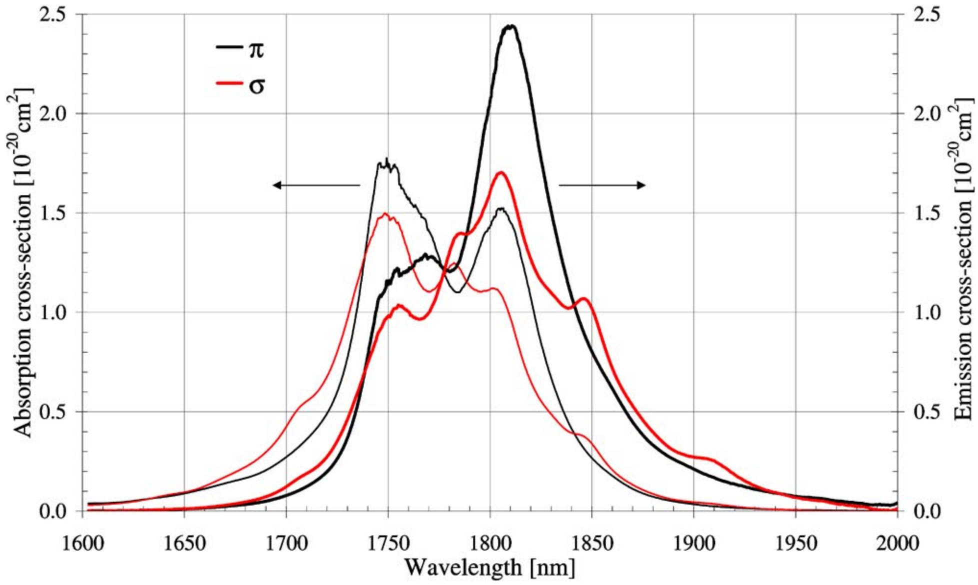

Fig. 1 The measured absorption cross sections (*thin*) and the calculated emission cross sections (*thick*) of Tm:GdVO$_4$ for π-polarised and σ-polarised light between 1600 and 2000 nm

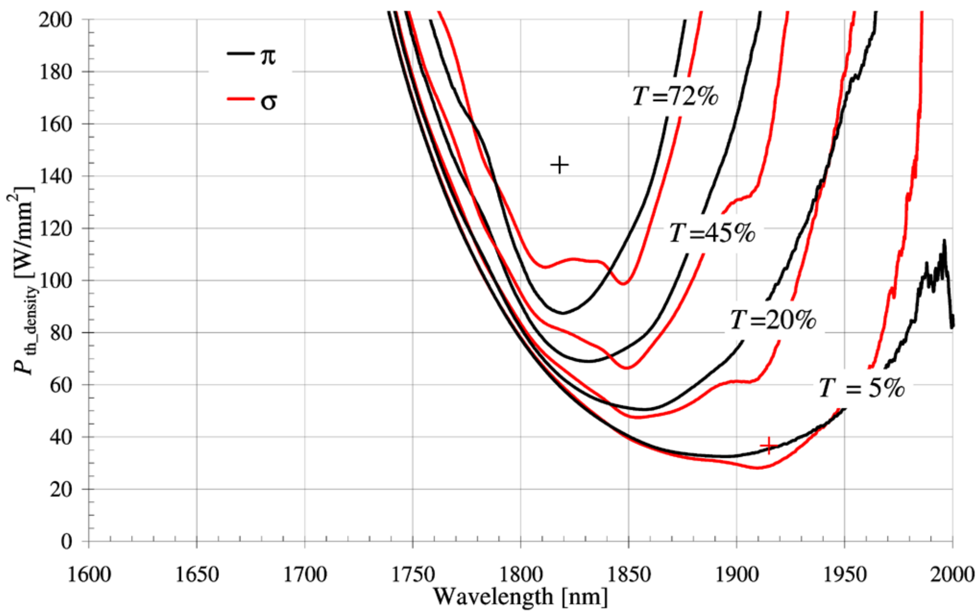

Fig. 2 The calculated Tm:GdVO$_4$ laser threshold power density at output coupling values T as a function of wavelength. The *two crosses* on the graph indicate the experimentally measured wavelength and incident threshold power density of the two demonstrated Tm:GdVO$_4$ lasers

features at 1850 and 1910 nm, as depicted in Fig. 1, are expected to play a major role in the predictions of oscillation wavelength, polarisation and threshold values for the Tm:GdVO$_4$ laser at typical output coupler values. Based on these calculations, the laser resonator configuration and desired pump beam sizes were designed.

3 Experimental set-up

For the initial laser experiments the 3% (at.) doped Tm:GdVO$_4$ crystal with dimensions $2.5 \times 2.5 \times 3$ mm^3 was used; it was anti-reflection coated for the pump wavelength at 800 nm and the laser wavelength at 1.8–2.0 μm. The crystal was wrapped in indium foil and clamped in a water-cooled copper mount thus providing conduction cooling from all four sides. The water temperature was controlled at 20°C.

The crystal was pumped with a fibre-coupled laser diode from one end only, as indicated by the schematic diagram in Fig. 3. The laser diode was operated in a quasi-continuous-wave (QCW) mode with 60 W maximum peak power incident on the crystal during the on time of the pump pulse, which was initially set to 20 ms at 5 Hz repetition rate. The pump duty cycle, together with the measured average pump power or average laser output power, was used to calculate the peak pump power and peak laser power, respectively. The centre wavelength of the laser diode was mea-

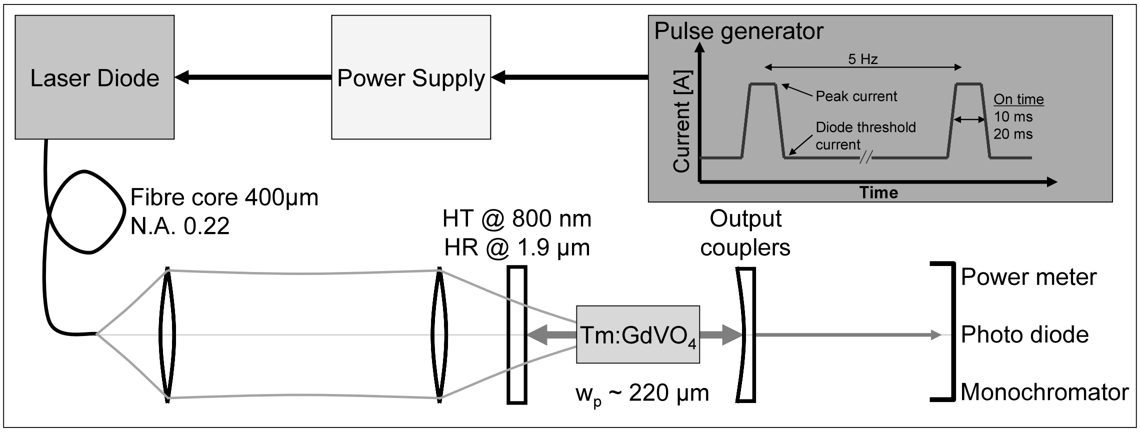

Fig. 3 The experimental set-up of the quasi-continuous-wave $Tm:GdVO_4$ laser

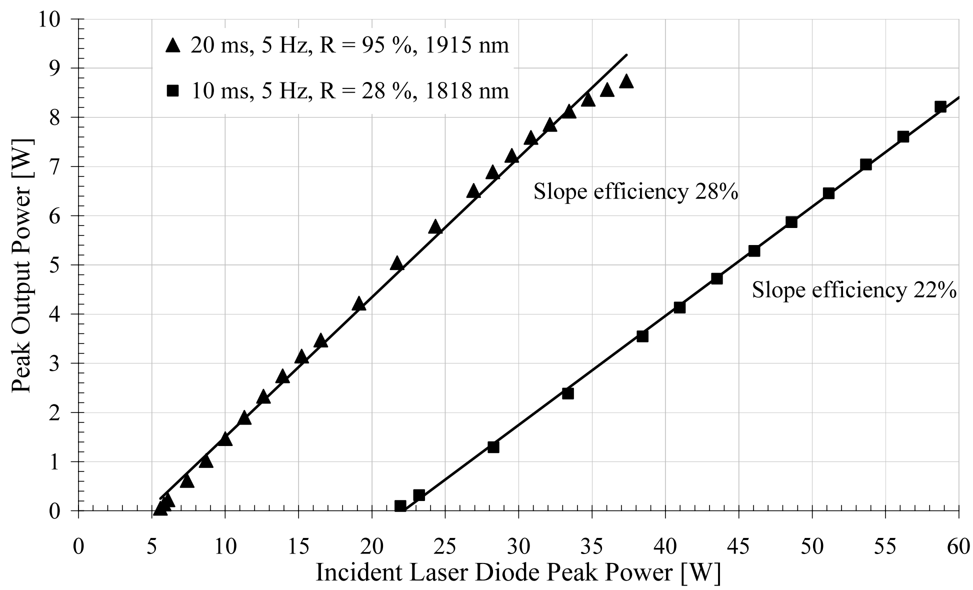

Fig. 4 The peak output power of the $Tm:GdVO_4$ laser with the $R = 95\%$ output coupler and with the $R = 28\%$ output coupler

sured to be 804 nm with the laser diode temperature controlled at 25°C. With one collimating lens and one focussing lens, the far-field image of the 400 µm core diameter fibre output (NA 0.22) was focussed into the crystal creating a bell-shaped beam profile with a minimum radius of approximately 220 µm.

The resonator was based on an elementary plano-concave design with a plane high-reflector (HR) end mirror, which was also coated for high transmission (HT) at the pump wavelength. The length of the resonator was approximately 26 mm, which together with the radius of curvature of the output coupler mirror defined a fundamental laser mode size in the crystal that closely matched the pump beam size. The resonator length was adjusted under lasing conditions to compensate for the thermal lens generated in the laser crystal. Two output coupler mirrors were available for the experiments. The output coupler employed in the first set of experiments had 95% reflectivity at 1.9 µm with 300-mm radius of curvature. The second output coupler had 55% reflectivity at 1.9 µm dropping to 28% at 1.82 µm. The radius of curvature of the second output coupler was 250 mm.

4 Experimental results

The centre wavelength of the $Tm:GdVO_4$ laser with the 95% reflectivity output coupler operating on σ-polarisation was measured to be 1915 nm, with ± 2.5 nm measurement uncertainty of the monochromator used in the experiment. The QCW output of the laser was observed to follow the pump pulse which had an on time of 20 ms at 5 Hz repetition rate. The threshold peak pump power was 5.6 W, which corresponded to a power density of 37 W/mm^2, which are values very close to those predicted earlier based on the threshold calculations as seen in Fig. 2. The plot of the $Tm:GdVO_4$ laser output power against the diode pump power incident on the crystal is shown in Fig. 4. The measured maximum laser peak power during the pulse was 8.7 W for 37.3 W of incident pump power on the laser crystal corresponding to an output energy of 175 mJ per pulse. Increasing the pump power beyond this point resulted in laser damage to the exit face of the crystal. The measured slope efficiency was 28.4% and the optical-to-optical efficiency was 23.4%. The intensity beam profile was measured throughout all the experiments which indicated a round beam with Gaussian intensity profile. No deterioration in beam quality was observed in the beam profile while scaling up the Tm:$GdVO_4$ laser output power.

In the next series of experiments, the output coupler with low reflectivity (55% at 1.9 μm and 28% at 1.82 μm) was used in an effort to reduce the intra-cavity power density, and the on time of the pump pulse was shortened to 10 ms to reduce the thermal load in the laser crystal. The damaged crystal was replaced with a crystal of similar doping concentration and dimensions. The centre wavelength of the second Tm:$GdVO_4$ laser was measured to be 1818 nm with ±2.5 nm measurement uncertainty. The threshold peak pump power was much higher, at 21.9 W, corresponding to a threshold power density of 144 W/mm^2. It was also observed that the laser polarisation was perpendicular to the Tm:$GdVO_4$ laser with the 95% output coupler, therefore operating on π-polarisation.

The maximum QCW output power of the Tm:$GdVO_4$ laser with the 28% reflectivity output coupler was observed to be 8.4 W at full diode pump power corresponding to 84 mJ per pulse. At this wavelength of 1818 nm, the slope efficiency was 22.2% and the overall laser efficiency was 14% of the incident laser diode power. At this low duty cycle of 5% on time, the output energy was limited by the available pump power. However, by increasing the pump pulse on time to 20 ms (duty cycle of 10%), the thermal fracture limit was reached at ~50 W of peak incident power due to the increased thermal load in the crystal. Up to the point of fracture, the slope efficiency was comparable to the 5% duty cycle case as was the threshold power density.

The measured wavelength and polarisation state agree very well with the predictions presented in Fig. 2. The small discrepancy between the calculated and the measured threshold power density values is most probably caused by additional losses induced in the laser cavity by thermal effects in the laser crystal before threshold is reached, and possibly upconversion losses [13], which are not incorporated in the calculations. The thermal lens, which is pump power dependent, also influences the laser mode size thereby invalidating the assumption that $w_l \approx w_p \approx w$. Furthermore, the increased heat load with stronger pumping causes a higher crystal temperature which subsequently increases the three-level nature of the Tm^{3+} laser. Nevertheless, it is clear that the calculations provide accurate predictions of the experimentally observed laser wavelength and polarisation.

Continuous-wave (CW) laser operation was also achieved, albeit with the laser-damaged crystal and the $R = 95\%$ output coupler. Operating in a CW mode with more than 1 W of output power resulted in thermal fracture of the laser crystal, at approximately 10 to 15 W of pump power. Due to the fractured crystal, a detailed analysis of the CW laser could not be conducted.

5 Conclusion

We have shown, based on detailed spectroscopic data which we measured for Tm:$GdVO_4$, that reliable calculations can be made of the expected output parameters of a diode-end-pumped Tm:$GdVO_4$ laser. The measured laser threshold, polarisation and wavelength were very close to the expected values for the laser with a 5% transmission output coupler. Also with a 72% transmission output coupler, the wavelength and polarisation of the Tm:$GdVO_4$ laser can be accurately predicted. We have shown and experimentally verified that this Tm:$GdVO_4$ laser can be efficiently operated with multi-watt output at the short wavelength of 1818 nm merely through the selection of a high output coupling value making it the first time that multi-watt operation at 1818 nm is achieved with a Tm:$GdVO_4$ laser. To our knowledge, this is also the shortest wavelength reported for a diode-pumped Tm-doped solid-state laser without the use of intra-cavity tuning elements. The maximum QCW output power was 8.7 W and the energy per pulse was 175 mJ. It is unclear why thermal fracture occurred at relatively low pump power. Possible reasons could be material quality or fundamental processes such as upconversion, or impurities in the laser crystals leading to excessive heat load and thermal fracture [13]. Further work on scaling Tm:$GdVO_4$ lasers will require investigation into these processes.

References

1. Chr.P. Wyss, W. Lüthy, H.P. Weber, V.I. Vlasov, Yu.D. Zavartsev, P.A. Studenikin, A.I. Zagumennyi, I.A. Shcherbakov, Opt. Commun. **153**, 63–67 (1998)
2. R. Lisiecki, P. Solarz, G. Dominiak-Dzik, W. Ryba-Romanowski, M. Sobczyk, P. Černý, J. Šulc, H. Jelínková, Y. Urata, M. Higuchi, Phys. Rev. B **74**, 035103 (2006)
3. E. Sorokin, I.T. Sorokina, A.N. Alpatiev, A.I. Zagumennyi, I.A. Shcherbakov, Tunable efficient continuous-wave room-temperature Tm^{3+}:$GdVO_4$ laser, in *Advanced Solid-State Lasers*, ed. by M. Fermann, L. Marshall, Trends in Optics and Photonics Series, vol. 68 (Optical Society of America, 2002), paper WA2
4. A.I. Zagumennyi, Y.D. Zavartsev, P.A. Studenikin, V.I. Vlasov, I.A. Shcherbakov, C.P. Wyss, W. Luthy, H.P. Weber, P.A. Popov, Quantum Electron. **29**(4), 298–300 (1999)
5. Y. Sato, T. Taira, Opt. Express **14**, 10528–10536 (2006)
6. Y.-F. Li, B.-Q. Yao, Y.-M. Liu, Y.-Z. Wang, Y.-L. Ju, Chin. Phys. Lett. **24**, 724–726 (2007)

7. P. Černý, H. Jelínková, Developing thulium lasers for depth-selective scalpels. http://spie.org/x8689.xml?highlight=x2416
8. S.A. Payne, L.L. Chase, L.K. Smith, W.L. Kway, W.F. Krupke, IEEE J. Quantum Electron. **28**(11), 2619–2630 (1992)
9. T.Y. Fan, R.L. Byer, IEEE J. Quantum Electron. **23**(5), 605–612 (1987)
10. R.C. Stoneman, L. Esterowitz, IEEE J. Sel. Top. Quantum Electron. **1**(1), 78–81 (1995)
11. J. Šulc, P. Koranda, P. Černý, H. Jelínková, Y. Urata, M. Higuchic, W. Ryba-Romanowski, R. Lisiecki, P. Solarz, G. Dominiak-Dzik, M. Sobczyk, Tunable lasers based on diode pumped Tm-doped vanadates Tm:YVO_4, Tm:$GdVO_4$, and Tm:$LuVO_4$, in *Solid State Lasers XVII: Technology and Devices*, ed. by W.A. Clarkson, N. Hodgson, R.K. Shori, Proceedings of SPIE, vol. 6871 (2008), p. 68711V
12. A.A. Lagatsky, N.V. Kuleshov, V.P. Mikhailov, Opt. Commun. **165**, 71–75 (1999)
13. J. Šulc, P. Černý, H. Jelínková, W. Ryba-Romanowski, R. Lisiecki, P. Solarz, G. Dominiak-Dzik, Y. Urata, M. Higuchic, Tm-doped vanadates under pulsed pumping with variable duty cycle: impact on lasing and fluorescence, in *Solid State Lasers and Amplifiers III*, ed. by J.A. Terry, T. Graf, H. Jelínková, Proceedings of SPIE, vol. 6998 (2008), p. 69980T